

Notch-filtered adiabatic rapid passage for optically driven quantum light sources

Cite as: APL Photonics 7, 111302 (2022); <https://doi.org/10.1063/5.0090048>

Submitted: 02 March 2022 • Accepted: 17 October 2022 • Accepted Manuscript Online: 17 October 2022 • Published Online: 09 November 2022

G. R. Wilbur, A. Binai-Motlagh,  A. Clarke, et al.



View Online



Export Citation



CrossMark

ARTICLES YOU MAY BE INTERESTED IN

[On-chip optical comb sources](#)

APL Photonics 7, 100901 (2022); <https://doi.org/10.1063/5.0105164>

[Nonlinear chirped interferometry for frequency-shift measurement and \$\chi^{\(3\)}\$ spectroscopy](#)

APL Photonics 7, 116103 (2022); <https://doi.org/10.1063/5.0109265>

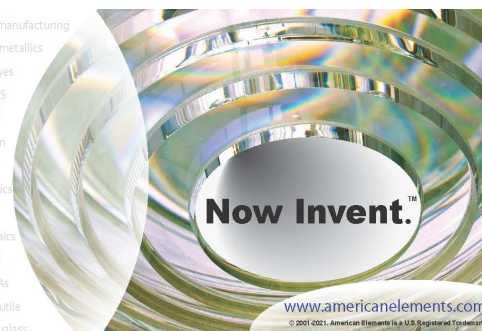
[Quantum dots as potential sources of strongly entangled photons: Perspectives and challenges for applications in quantum networks](#)

Applied Physics Letters 118, 100502 (2021); <https://doi.org/10.1063/5.0038729>



yttrium iron garnet glassy carbon beamsplitters fused quartz additive manufacturing
zeolites III-IV semiconductors gallium lump copper nanoparticles organometallics
nano ribbons barium fluoride europium phosphors photonics infrared dyes
epitaxial crystal growth ultra high purity materials transparent ceramics CIGS
cerium oxide polishing powder cermet nanodispersions
surface functionalized nanoparticles MRE grade materials thin film
OLED lighting solar energy
sputtering targets fiber optics
h-BN deposition slugs
CVD precursors photovoltaics
metamaterials borosilicate glass
YBCO superconductors InGaAs
indium tin oxide MgF2 rutile
diamond micropowder optical glass

The Next Generation of Material Science Catalogs



Notch-filtered adiabatic rapid passage for optically driven quantum light sources

Cite as: APL Photon. 7, 111302 (2022); doi: 10.1063/5.0090048

Submitted: 2 March 2022 • Accepted: 17 October 2022 •

Published Online: 9 November 2022





View Online



Export Citation



CrossMark

G. R. Wilbur,¹ A. Binai-Motlagh,¹ A. Clarke,¹  A. Ramachandran,¹ N. Milson,¹ J. P. Healey,¹ S. O'Neal,^{2,a)}
D. G. Deppe,^{2,b)} and K. C. Hall^{1,c)} 

AFFILIATIONS

¹Department of Physics and Atmospheric Science, Dalhousie University, Halifax, Nova Scotia B3H 4R2, Canada

²The College of Optics and Photonics, University of Central Florida, Orlando, Florida 32816-2700, USA

^{a)}Present address: Imec, Kissimmee, Florida 34744, USA.

^{b)}Present address: SdPhotonics, Richardson, Texas 75081, USA.

^{c)}Author to whom correspondence should be addressed: Kimberley.Hall@dal.ca

ABSTRACT

We present a driving scheme for solid-state quantum emitters, referred to as Notch-filtered Adiabatic Rapid Passage (NARP), that utilizes frequency-swept pulses containing a spectral hole resonant with the optical transition in the emitter. NARP enables high-fidelity state inversion and exhibits robustness to variations in the laser pulse parameters, benefits that are derived from the insensitivity of the condition for adiabatic evolution. NARP also offers the advantage of immunity to phonon-mediated excitation-induced dephasing when positively chirped control pulses are used. Our resonant driving approach could be combined with spectral filtering of the scattered pump light and photonic devices for enhanced collection efficiency to realize simultaneous high indistinguishability and brightness in single photon source applications.

© 2022 Author(s). All article content, except where otherwise noted, is licensed under a Creative Commons Attribution (CC BY) license (<http://creativecommons.org/licenses/by/4.0/>). <https://doi.org/10.1063/5.0090048>

I. INTRODUCTION

Deterministic sources of single photons are required for a number of emerging areas in quantum information science and technology, including photonic quantum computing and simulation,^{1,2} quantum repeaters and networks,^{3–5} and quantum-enhanced sensing and metrology.^{6–9} For such applications, the ideal quantum emitter would be capable of producing a single photon on-demand with successive photons being indistinguishable in all its degrees of freedom. For solid-state quantum emitters based on semiconductor quantum dots (QDs), considerable improvements in emission properties have been achieved in recent years,^{10–41} yet the simultaneous achievement of high photon brightness and indistinguishability remains a challenge. For the highest degree of indistinguishability, resonant pumping of the quantum emitter is ideal since non-resonant excitation can lead to timing jitter due to incoherent relaxation pathways and spectral wandering associated with unwanted excess charges in the vicinity of the emitter.^{11,12,15,16,27,40–42} Resonant pumping, however, necessitates an

efficient approach to separating the scattered excitation light from the emitted photon stream.

The resonance fluorescence from the emitter may be separated from the excitation laser using crossed-polarized excitation and detection,^{11–17} but this approach limits the maximum brightness to 50% even if all other sources of loss are minimized.^{13,35,37,40,43–48} The near-resonant excitation assisted by phonons^{28–30} enables spectral isolation of the emission from the pump laser but relies on incoherent relaxation processes that reduce coherence. In two-photon excitation schemes, the pump light and fluorescence are also nondegenerate due to the nonzero biexciton binding energy;^{31–39} however, the time correlation between the biexciton and exciton emission and the lack of a single polarization tied to the biexciton cascade limit the indistinguishability with this approach.^{49–51} Polarization-sensitive optical microcavities^{18,19} and waveguide modes^{20–27} have also been utilized in recent years to address the need to separate the excitation light and emitted photoluminescence (PL). The efficiency of excitation and detection is limited in such schemes by the strength of coupling into the associated optical modes.

A few creative approaches to solving the trade-off between brightness and indistinguishability have emerged in recent years.^{52–54} These approaches rely on the insight that, in the nonlinear driving regime, coherent driving of a two-level system is possible in the absence of light resonant with the optical transition provided that the cancellation of the time-integrated Rabi frequency that normally occurs with off-resonant driving is incomplete. One method uses a bichromatic laser pulse with spectral components on either side of the optical transition but with a node on-resonance.^{52,53} In such a case, the time-integrated pulse area is nonzero, provided that the symmetry is broken between the red and blue driving conditions, which is naturally caused by phonon-mediated excitation processes and can be enhanced by making the two spectral components have unequal strengths.⁵³ This approach enables background-free single photon extraction using a simple bandpass filter resonant with the optical transition, but the maximum inversion is limited to 60%. Another pumping scheme referred to as swing-up⁵⁴ was recently proposed in which the positive and negative cycles of the Rabi frequency are rendered inequivalent by using two spectral components tuned below the optical transition that beat together. Excitation of the emitter is possible in this case because the cancellation effects present under non-resonant pumping are incomplete such that the system reaches inversion after many Rabi cycles. For both of these pumping schemes, the final inversion of the emitter is sensitive to the pulse parameters, making practical implementation difficult.

Here, we show that inversion of a quantum emitter may be achieved using a frequency-swept pulse subjected to a notch filter resonant with the optical transition in the emitter, enabling the simultaneous requirements of coherent driving of the emitter and the spectral isolation of the emitted photons from the excitation pulse. This NARP scheme exploits adiabatic transfer of the system through an anticrossing in the dressed states of the optically driven emitter, making it intrinsically robust to fluctuations in the laser pulses and to variations in the optical properties of the quantum emitters often present in solid-state systems. Furthermore, the use of positively chirped pulses suppresses phonon-mediated excitation-induced dephasing^{55–61} that has been shown to limit the final inversion for many of the above-mentioned excitation schemes.^{53,54} We demonstrate our pumping scheme experimentally in a single semiconductor QD, but our approach would be applicable to a wide range of solid-state quantum emitter systems.⁶²

II. THE NARP SCHEME

The optical excitation scheme presented here is a modified version of adiabatic rapid passage (ARP), which utilizes a frequency-swept pulse to realize quantum state inversion.^{63–65} In ARP, the laser pulse is linearly chirped, with an electric field given by $E(t) = \frac{1}{2}E_p(t) \exp[-i(\omega_l t + \alpha t^2)]$, where $E_p(t)$ is the pulse envelope, ω_l is the center frequency of the laser pulse, and α is the temporal chirp. The instantaneous detuning of the laser frequency from the transition frequency of the quantum emitter (ω_0) is time-dependent, given by $\Delta(t) = \Delta_0 - 2\alpha t$ with a static detuning of $\Delta_0 = \omega_0 - \omega_l$, which may be nonzero in the general case, such that the frequency of the pulse is swept from below resonance to above resonance or vice versa depending on the sign of the chirp α . The

dressed states of the system in the presence of the light field ($|\Psi_{\pm}\rangle$) correspond to superpositions of the bare ground and excited states of the emitter ($|0\rangle$ and $|1\rangle$, respectively) with coefficients that evolve in time during the pulse from purely $|0\rangle$ to $|1\rangle$ or vice versa. The energy splitting between the dressed states is $\sqrt{\Omega(t)^2 + \Delta(t)^2}$, where $\Omega(t) = \frac{\mu E_p(t)}{\hbar}$ is the Rabi frequency, and μ is the dipole moment of the optical transition. In the limit that $|\Delta \frac{d\Omega}{dt} - \Omega \frac{d\Delta}{dt}| \ll [\Omega^2 + \Delta^2]^{\frac{3}{2}}$ ⁶⁵ is satisfied, the control process is adiabatic and the system remains in one of the dressed states while the state itself reverses character, leading to inversion. The initial state of the system, together with the sign of the pulse chirp, dictates whether the system traverses the anticrossing in $|\Psi_+\rangle$ or $|\Psi_-\rangle$.

ARP is an intrinsically robust control process because the condition for adiabatic state transfer may be satisfied under a wide range of conditions. The dipole moment and transition frequency of the emitter can vary in ensembles of emitters in solid-state systems due to differences in the environment around each emitter.⁶² In addition, the laser system used to drive the emitter can fluctuate in both intensity (leading to changes in the pulse area $\theta = \int_{-\infty}^{\infty} \frac{\mu E_p(t)}{\hbar} dt$) and the laser central frequency ω_l causing changes in Δ_0 . For ARP, the adiabatic condition may be satisfied in the presence of such variations such that high-fidelity inversion is maintained.^{63–66} Furthermore, the choice of the positive chirp in the laser pulses used to drive the emitter leads to inversion via the lower-energy dressed state, which suppresses phonon-induced dephasing processes at low temperatures in contrast to other driving schemes.⁵⁶ Robust inversion has been demonstrated using ARP in solid-state emitters based on excitons in semiconductor QDs in recent years,^{56,66–72} including the driving of a triggered single photon source.¹⁰

In the NARP scheme, the frequency-swept pulse used to drive the quantum emitter is modified by implementing a mask function in the frequency domain that leads to a node in resonance with the optical transition in the emitter. Such a mask function could be realized by applying a standard dual-mask liquid-crystal array spatial light modulator (SLM) at the focal plane of a 4f pulse shaper configuration,^{73,74} as in Fig. 1(a). In this case, the total mask imposed by the shaping system is given by

$$M(\omega) = A(\omega)e^{i\Phi(\omega)}, \quad (1)$$

where the amplitude mask $A(\omega)$ introduces the spectral hole and the phase mask is given by $\Phi(\omega) = \frac{\phi''}{2}(\omega - \omega_0)^2$. The spectral chirp ϕ'' is related to the temporal chirp α by $\alpha = 2\phi''/[\tau_0^4/(2 \ln(2))^2 + (2\phi'')^2]$. In the theoretical simulations presented here, the amplitude mask was taken as $A(\omega) = 1 - e^{-\ln(2)(\omega - \omega_0)^2/\delta^2}$ with 2δ being the full-width-at-half-maximum (FWHM) of the spectral hole. This choice for $A(\omega)$ provides an exact spectral node on resonance with the quantum emitter with a form that provides a smooth analytic function for ease of numerical integration. In experiments, a square-shaped spectral hole is easier to implement (e.g., by turning off 1 or more pixels or using a physical blocker in front of the SLM) and would facilitate the synchronous driving of distinct emitters.

For application of NARP to triggered single photon sources, a bandpass filter can be used to block the pump light and pass

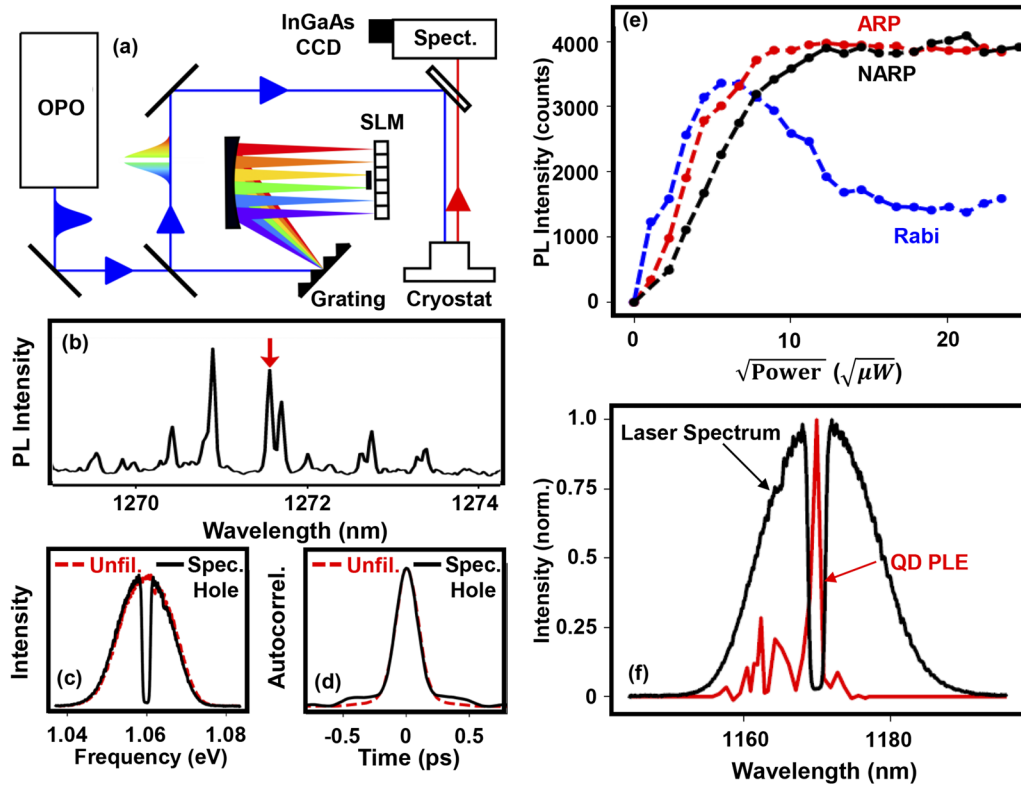


FIG. 1. (a) Schematic diagram of the quantum control apparatus. (b) Micro-PL showing the s-shell emission from individual QDs. The arrow indicates the QD used for the experiments. (c) Laser spectrum for the unfiltered pulse (red dashed curve) and the spectral hole pulse (black solid curve). (d) Measured pulse autocorrelation for the unfiltered pulse (red dashed curve) and the spectral hole pulse (black solid curve). (e) Measured PL intensity from a single semiconductor QD under optical driving by an unfiltered pulse with $\phi'' = 0$ (Rabi, blue symbols) and $\phi'' = 0.15 \text{ ps}^2$ (ARP, red symbols), and for a spectral hole pulse with a 3 meV hole and $\phi'' = 0.15 \text{ ps}^2$ (NARP, black symbols). (f) Laser spectrum for the spectral hole pulse (black curve) together with the photoluminescence excitation (PLE) spectrum of the QD used in the experiments (red curve).

the emitter fluorescence with near unity efficiency. As we show here, the condition for adiabatic transfer through the anticrossing and concomitant inversion of the quantum emitter may still be achieved in the presence of a spectral hole centered on the emitter transition.

III. THEORETICAL MODEL

The Hamiltonian of a two-level system interacting with a pulsed laser field $E(t) = g(t) \cdot \cos(\omega_0 t + \phi(t))$ in the rotating wave approximation is given by

$$H = -\hbar \frac{\delta}{2} \sigma_z + \frac{\hbar}{2} (\text{Re}\{\Omega(t)\} \sigma_x + \text{Im}\{\Omega(t)\} \sigma_y). \quad (2)$$

Here, $\Omega(t) = \frac{\mu g(t)}{\hbar} e^{i\phi(t)}$ is the complex Rabi frequency. μ is the dipole moment of the transition, and $g(t)$ is the envelope of the pulse. The dynamics can be described by the Bloch vector $\vec{S} = (u, v, w)$ with the time evolution governed by the Bloch equation,

$$\dot{\vec{S}} = \vec{S} \times \vec{\Lambda}, \quad (3)$$

where

$$\vec{\Lambda} = (-\text{Re}\{\Omega(t)\}, -\text{Im}\{\Omega(t)\}, \Delta)/2. \quad (4)$$

The effect of the 4f pulse-shaper can be described as follows:

$$E_{out}(t) = \mathcal{F}^{-1}(\mathcal{F}(E_{in}(t)) \cdot M(\omega)), \quad (5)$$

where $M(\omega)$ is given by Eq. (1) and \mathcal{F} denotes the Fourier transform. $E_{in}(t)$ is the input pulse after dispersion compensation (which we take to be a Gaussian $E_0 e^{-2 \ln(2)t^2/\tau_0^2}$), and $E_{out}(t)$ is the pulse coming out of the 4f system. The impact of the amplitude and phase masks on the laser pulse characteristics is shown in Fig. 2.

The NARP scheme is very general and may be applied to a whole host of physically distinct quantum emitters beyond solid-state platforms. In semiconductor quantum dots, the dominant dephasing channel limiting inversion of the system is decoherence tied to deformation potential coupling to LA phonons. Our calculations use a density matrix approach with electron-LA phonon coupling included, following the model developed in Ref. 75. The QD wave functions were taken as the s-shell solutions to the three-dimensional simple harmonic oscillator. The equation of motion

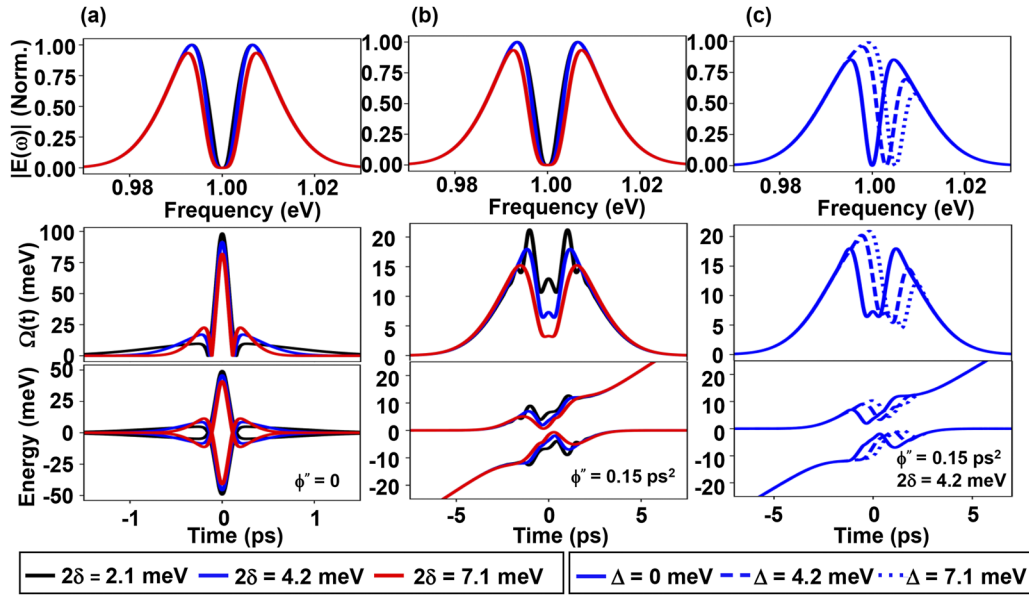


FIG. 2. Calculated pulse characteristics showing the differing impacts of the amplitude mask $A(\omega)$ and phase mask $\Phi(\omega)$ on the amplitude and phase of the complex Rabi frequency $\Omega(t)$ for the driving pulse used for ARP. Calculated pulse spectrum (top), Rabi frequency (middle) and dressed state energies (bottom) for (a) the amplitude mask only ($\phi'' = 0$) and (b) both the amplitude and phase mask ($\phi'' = 0.15 \text{ ps}^2$) for different values of 2δ and a fixed pulse area of 7π . The dominant impact of $A(\omega)$ is to create wings in $|\Omega(t)|$. The quadratic form of $\Phi(\omega)$ leads to a quadratic phase vs time, representing a linearly-time-varying phase derivative, which corresponds to a sweep in the instantaneous frequency vs time (i.e., chirp). This chirp broadens the wings. Since $|\Omega(t)|$ does not vanish at any time during the anti-crossing, the condition for adiabaticity may still be satisfied for sufficiently large pulse area. (c) Same as (b), showing the case of an off-centre spectral hole. The results in (c) illustrate the general pulse characteristics for detuned pulses for which the spectral hole would be chosen to be resonant with the transition energy of the quantum emitter (see Fig. 4).

governing the evolution of the exciton's Bloch vector in the presence of phonons is

$$\begin{aligned} \dot{u} &= \Delta \cdot v - \left(\frac{\Delta \Omega}{\Lambda^2} \right) \text{Re}[K(\Lambda)]w - \frac{\pi \Omega J(\Lambda)}{2\Lambda} - \left(\frac{\Omega}{\Lambda} \right)^2 \text{Re}[K(\Lambda)]u \\ \dot{v} &= -\Delta \cdot u + \Omega \left(1 + \frac{\text{Im}[K(\Lambda)]}{\Lambda} \right) w - \left(\frac{\Omega}{\Lambda} \right)^2 \text{Re}[K(\Lambda)]v \\ \dot{w} &= -\Omega \cdot v, \end{aligned}$$

where $J(\omega) = \eta \omega^3 \exp(-\omega/\omega_c)^2$ is the phonon spectral density, $K(\omega) = \int_0^\infty \tilde{K}(t) e^{i\omega t} dt$ and $\tilde{K}(t) = \int_0^\infty J(\omega) \coth\left(\frac{\hbar\omega}{2k_B T}\right) \cos(\omega t) d\omega$ are the phonon bath correlation functions. $\Lambda = \sqrt{\Omega^2(t) + \Delta^2(t)}$ is the generalized Rabi frequency. While this Markovian model neglects memory effects within the phonon bath, the additional terms in the kinetic equations tied to phonons are evaluated at the generalized Rabi frequency. The impact of phonon coupling is, therefore, determined by the characteristics of the laser pulse and varies with time during optical control. With the application of a positively chirped control pulse, the system evolves through the anticrossing in the lower-energy dressed state, which eliminates phonon-induced transitions between the dressed states for control at low temperature,^{56,72} thereby suppressing the impact of phonon-induced decoherence. This is a key advantage of both ARP and NARP for the optical driving of quantum emitters. Table I shows all the parameters used for the simulations.

TABLE I. Theoretical parameters used in the numerical simulations of the quantum state dynamics.

Parameter	Value
δ (meV)	3
μ (D)	25
ω_c (meV)	1.584
η (ps^2)	0.0272
τ (fs)	117
ω_0 (eV)	1.000

IV. EXPERIMENTAL METHODS

The solid-state quantum emitter system used here to demonstrate the NARP control scheme was a single InGaAs quantum dot. Optical control was carried out on the p-shell transition, with detection of the final quantum state via the s-shell photoluminescence emission (PL),⁷⁶ but our scheme could also be used for s-shell pumping, as was assumed in the theoretical calculations presented in Sec. V. A schematic diagram of the experimental apparatus is shown in Fig. 1(a). The InGaAs/GaAs quantum dot structure studied in this work was grown under conditions optimized to achieve an s-shell optical transition within the 0-band at a low temperature. The QD sample was held at 10 K in a cryostat equipped with an attocube nanopositioner. The laser source was a tunable infrared optical parametric oscillator with a pulse duration after dispersion

compensation of 110 fs. This corresponds to a spectral width of 18 meV, much smaller than the 85 meV separation between the s-shell and p-shell transitions. The laser pulse spectrum was centered on the p-shell transition (1170 nm determined using PL excitation measurements), as shown in Fig. 1(f). The s-shell PL centered at 1271.6 nm [arrow in Fig. 1(b)] was detected using a 0.75 m spectrometer equipped with a liquid nitrogen-cooled InGaAs array detector. The overall spectral resolution of the detection system is 30 μeV .

A 4f pulse shaper equipped with a dual mask 128-pixel SLM was used to introduce dispersion compensation and to impose the desired spectral chirp. For the amplitude mask, experiments were carried out using a 5 pixel blocking mask as well as a physical blocker in front of the SLM to create the spectral hole (a 24 AWG copper wire producing an amplitude mask of width 3 meV), with similar results. The experimental results in Fig. 1(e) were taken using the physical blocker. The laser pulse spectrum and autocorrelation

with and without the spectral hole are shown in Figs. 1(c) and 1(d). For additional details regarding the experimental techniques, see Ref. 69.

V. RESULTS

A. Simulations of the NARP scheme

The results of numerical simulations of quantum state dynamics illustrating the efficacy of the NARP scheme for quantum state inversion are shown in Figs. 3(a) and 3(b). These simulations were targeted at the situation of an optically driven single semiconductor QD and used a density matrix approach, taking into account deformation potential interactions with acoustic phonons.⁷⁵ Figures 3(a) and 3(b) show the occupation of the excited state as a function of pulse area for a range of values of positive pulse chirp for an unfiltered Gaussian spectrum [Fig. 3(a)] and a pulse

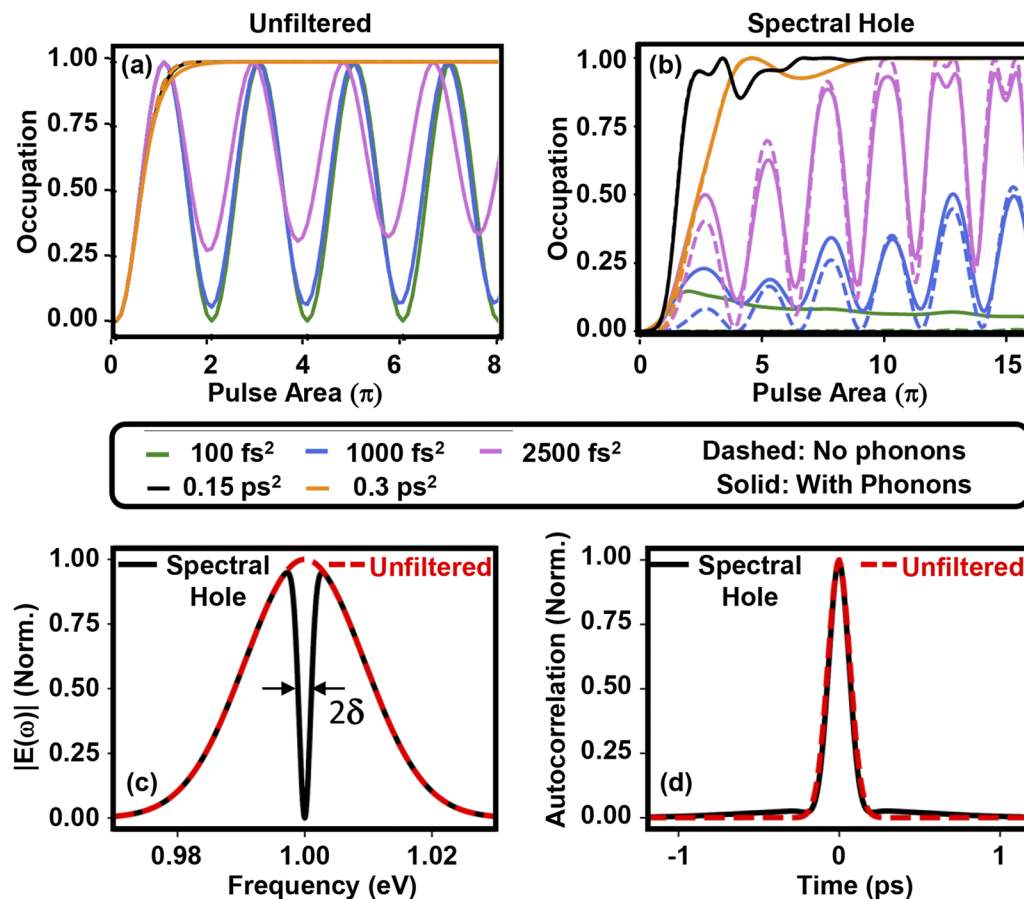


FIG. 3. (a) Results of calculations of the quantum state dynamics for optical driving of a single semiconductor QD with an unfiltered Gaussian laser pulse for different values of spectral chirp ϕ'' . (b) Same as (a) for a spectral hole pulse with $2\delta = 2.1$ meV. For chirps above the threshold for adiabatic state transfer (ϕ'' larger than 0.1 ps² for which $\alpha = 5$ ps⁻², $\tau_p = 2.3$ ps, and Δ spans ± 15 meV during the pulse), the system inverts via ARP in (a) and NARP in (b). In (a) and (b), the solid (dashed) curves indicate the calculated state dynamics with (without) coupling to LA phonons. (c) Laser spectrum for the Gaussian unfiltered pulse (red dashed curve) and spectral hole pulse (solid black curve). (d) Calculated pulse autocorrelation corresponding to the spectra in (c).

subjected to spectral filtering using the mask in Eq. (1) with $2\delta = 2.1$ meV [Fig. 3(b)], referred to as a spectral hole pulse. The corresponding pulse characteristics are shown in Figs. 3(c) and 3(d). For the unfiltered pulse, a transition from the Rabi rotation regime to the adiabatic regime is observed as ϕ'' is increased, consistent with previous work.^{10,56,66–72} Once the adiabatic regime is reached, which occurs for $\phi'' \gtrsim 0.1$ ps² and $\theta \gtrsim 2\pi$, the upper state occupation is insensitive to changes in pulse area, a key signature of adiabatic rapid passage and robust inversion. For the spectral hole pulse with $\phi'' = 0$, the occupation vanishes in the absence of phonon coupling because the time-integrated Rabi frequency is zero, as discussed previously for the case of unchirped pulses.⁵³ As shown in Fig. 3(b), the inclusion of phonons leads to a small but nonzero state occupation because phonons break the spectral symmetry of the driving conditions through the introduction of incoherent dynamics.⁵³ The results in Fig. 3(b) show that the use of frequency-swept pulses also serves to break the symmetry. The state occupation increases with an increasing ϕ'' . For low ϕ'' , the occupation vs pulse area resembles an imperfect Rabi rotation. For ϕ'' exceeding 0.1 ps², the adiabatic regime is reached. In this limit, for sufficiently large pulse area, the inversion process is robust to changes in pulse area for both the unfiltered pulse and the spectral hole pulse. Our simulations

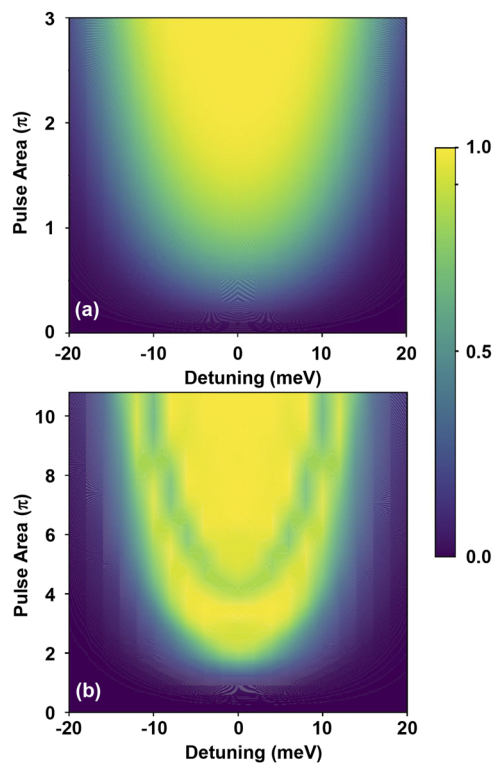


FIG. 4. Calculated upper state occupation as a function of pulse area and detuning of the center frequency of the laser pulse from the optical transition energy of the quantum dot exciton for an unfiltered Gaussian pulse (a) and a spectral hole pulse with $2\delta = 2.1$ meV (b). These results illustrate the robustness of inversion with optical driving using both ARP and NARP. The pulse spectral chirp is 0.15 ps².

also indicate the robustness of NARP to laser detuning (Fig. 4), as demonstrated previously for ARP.⁶⁶

We can gain insight into the quantum state dynamics from the energies of the dressed states of the optically driven system (E_{\pm}), which are shown in Fig. 5(a). Robust inversion occurs for frequency-swept pulses with or without a spectral hole because in both cases, the adiabatic condition for quantum state transfer is satisfied. The introduction of the spectral hole leads to structure in the temporal shape of the pulse, as shown in Fig. 5(b), which has the effect of increasing the threshold pulse area for NARP. Calculations as a function of the hole width (δ) (see Fig. 6) indicate that the primary cause of this increase is the transfer of energy into the wings of the pulse, which reduces the size of the Rabi frequency at time $t = 0$, thereby reducing the magnitude of the dressed-state splitting at the anticrossing. The adiabatic condition $|\Delta \frac{d\Omega}{dt} - \Omega \frac{d\Delta}{dt}| \ll [\Omega^2 + \Delta^2]^{\frac{3}{2}}$ is then recovered for larger θ , with a threshold pulse area that increases with increasing δ . Nevertheless, for a given value of δ and a sufficiently large pulse area, robust inversion occurs. The corresponding quantum state dynamics using a Bloch vector representation are shown without phonon coupling in Figs. 5(c) and 5(d). For excitation with the spectral hole pulse with $\phi'' = 0$, no net excitation occurs due to the zero time-integrated Rabi frequency. For chirped pulse excitation, robust inversion of the quantum emitter is realized for either traditional ARP or NARP, with only a slight modification of the trajectory in the latter case.

The results in Fig. 1(b) indicate that the fractional change in the occupation resulting from the impact of phonons diminishes as the chirp is increased. This reflects the use of positively chirped pulses, which suppress LA phonon-mediated transitions between the dressed states within the adiabatic regime at low temperatures.⁷⁴ In Fig. 3(b), the dashed and solid curves coincide for ϕ'' and θ above the threshold for ARP, indicating that phonons have no influence on quantum state dynamics in this limit. Our results therefore indicate that all of the advantages of ARP for optical inversion of quantum emitter systems, including the ability to suppress decoherence tied to phonons and the robustness of the inversion process to fluctuations in the laser source, are maintained for the NARP scheme.

B. Experimental demonstration of quantum state inversion using the NARP scheme

The results of optical control experiments on a single QD using the NARP scheme are shown in Fig. 1(e). The PL intensity vs the square root of the excitation power, which is proportional to the pulse area, is shown for an unfiltered pulse with zero chirp (Rabi, blue symbols), for an unfiltered pulse with $\phi'' = 0.15$ ps² (ARP, red symbols) and for the spectral hole pulse with $\phi'' = 0.15$ ps² (NARP, black symbols). For the unfiltered pulse with zero chirp, a damped Rabi rotation is observed. For excitation by the chirped, unfiltered pulse, the PL intensity saturates at a constant value for pulse areas above the threshold for ARP, as observed in prior experiments on similar QDs.^{10,66–72} For the chirped spectral hole pulse, the exciton inversion also exhibits a saturation behavior. For chirped pulse excitation, the pulse area required to reach full inversion is $\sim 30\%$ larger for the NARP pulse than the ARP pulse. The findings in Fig. 1(e) are in qualitative agreement with the theoretical predictions in Fig. 3.

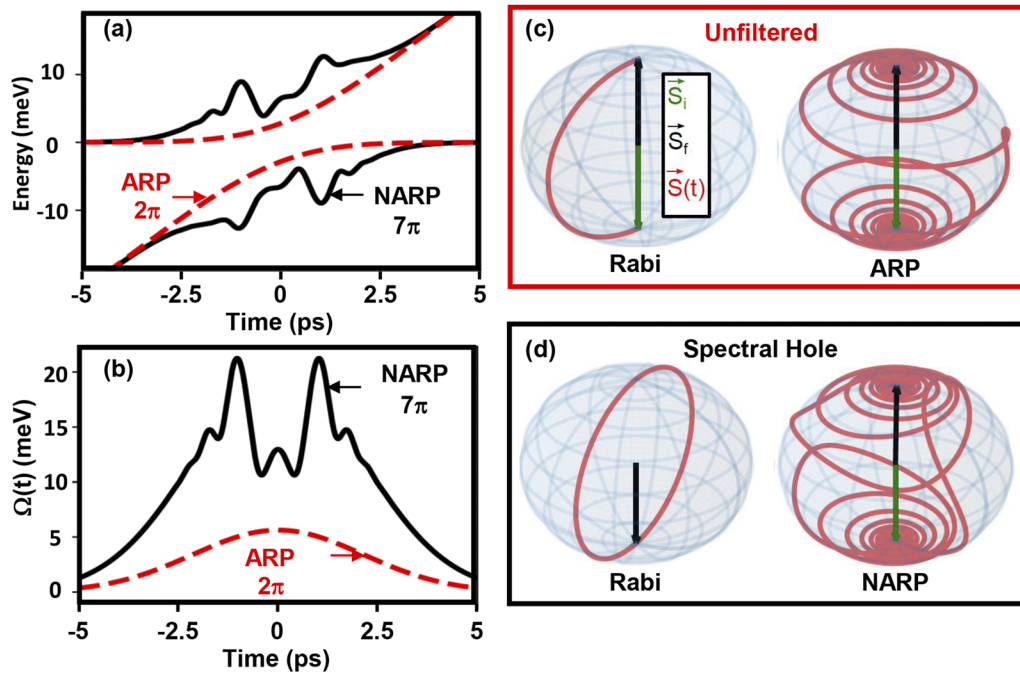


FIG. 5. (a) Energies E_{\pm} of the dressed states $|\Psi_{\pm}\rangle$ for an ARP pulse (dashed red curve) and a NARP pulse with $2\delta = 2.1$ meV (solid black curve) for $\phi'' = 0.15$ ps². (b) Calculated Rabi frequency as a function of time corresponding to the dressed state energies in (a). The pulse areas in (a) and (b) were chosen as the minimum values leading to robust inversion, corresponding to 2π (7π) for the ARP (NARP) pulse. (c) Quantum state dynamics depicted on the Bloch sphere for an unfiltered Gaussian pulse with $\phi'' = 0$ and a pulse area of $\theta = \pi$ (left) and $\phi'' = 0.15$ ps² with $\theta = 3.4\pi$ (right). (d) Bloch spheres for a spectral hole pulse with $2\delta = 2.1$ meV for $\phi'' = 0$ and a pulse area of $\theta = 3.4\pi$ (left) and $\phi'' = 0.15$ ps² with $\theta = 3.4\pi$ (right).

The observed increase in the threshold pulse area in the experiments was smaller than in the theoretical simulations, likely reflecting the different shapes of $A(\omega)$ and associated differences in the pulse temporal structure.

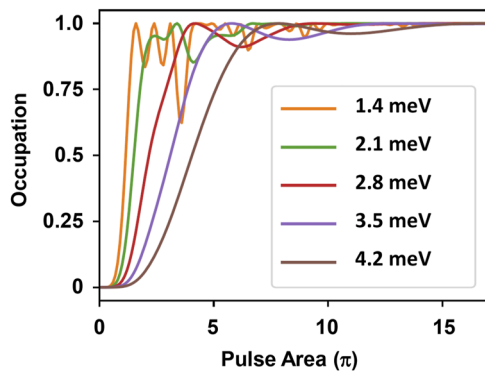


FIG. 6. (a) Calculated upper state occupation as a function of pulse area for different full-width-at-half-maximum hole widths (2δ). The optimum value of 2δ would be determined in practice by the range of transition energies of emitters being driven synchronously by the same NARP pulse.

VI. DISCUSSION

For single photon source applications, a variety of experimental approaches have been used to eliminate the trade-off between indistinguishability and brightness, which together require resonant driving of the two-level system in the quantum emitter and the efficient separation of the emitted photon stream from the scattered pump light. The NARP scheme allows one to simultaneously satisfy these two requirements, removing the trade-offs present in other approaches and setting the stage for high-performance single photon sources. For the results in Fig. 3, the ground-state optical transition in the emitter was driven with a NARP pulse possessing an exact node on resonance. There is therefore no fundamental limit to the efficiency of spectral isolation of the emitted photon stream from the scattered laser light. When applying NARP in practice, one may use a notch filter to create the spectral node and a high-efficiency bandpass filter to reject the scattered pump light, for which commercially available options exist with an OD > 6 and a transmission of 98%.⁷⁷ One may obtain an estimate of the potential performance of our scheme by assuming the notch (bandpass) filter has a bandwidth of 4 meV (1 meV). Assuming an optimized photonic structure is used to maximize optical coupling to the quantum dot, the driving laser power for a π pulse may be reduced to 1.6 μ W.⁷⁸ If two notch filters each with an OD6 are applied to the driving laser pulse, with a single bandpass filter with an OD7, the scattered pump

light is dominated by wavelengths outside the notch at a level of 7×10^{-3} photons/pulse. With two stacked bandpass filters, the scatter is dominated by wavelengths inside the passband at a level of 5×10^{-9} photons per pulse, a value that could be further reduced by reducing the width of the passband relative to the notch filter bandwidth or by applying an additional filter. Assuming a transmission of the passband filter of 98%, reflecting commercially available filters, this would give a loss of 2%–4% in the above scenarios, far superior to the minimum 50% loss associated with polarization filtering approaches.

Our pumping scheme enables a maximum inversion efficiency of unity, in contrast to the limit of 0.6 for unchirped bichromatic pulses.^{52,53} Our scheme also allows for suppression of LA-mediated dephasing, representing a significant advantage over phonon-assisted pumping,^{79,80} bichromatic driving,^{52,53} and swing up⁵⁴ schemes. In addition, unlike the bichromatic or swing-up schemes, NARP is insensitive to the details of the driving pulse (pulse area, magnitude of chirp, width of spectral hole). The use of robust inversion via NARP and static spectral filters offers simplicity over time-based gating approaches for isolating the single photon stream. Our findings indicate that a spectral hole width as large as several meV may be used to invert the emitter with a modest increase of 30% in driving pulse area. This would enable the parallel excitation of multiple emitters with unequal transition energies as long as these transitions fall within the filtered band,⁶⁶ adding versatility for application of our approach in real solid-state emitter systems.

VII. CONCLUSIONS

In summary, we present an optical driving scheme for solid-state quantum emitter systems that utilizes spectrally modified, frequency-swept laser pulses. Our findings indicate that the adiabatic regime for quantum state inversion may still be reached in the presence of a spectral hole coincident with the optical transition in the quantum emitter with only a modest increase in pulse area relative to traditional ARP. Our NARP scheme would enable $\lesssim 10^{-8}$ scattered photons per emitted photon with only a 4% detection loss using standard commercial filters while retaining all of the benefits of ARP, including insensitivity to fluctuations in the driving laser pulse and the ability to suppress phonon-mediated dephasing processes. We demonstrate NARP experimentally in a single InGaAs semiconductor QD. The use of the driving scheme we present here in conjunction with photonic cavity geometries to enhance collection efficiency would enable the realization of quantum emitters with simultaneous high photon indistinguishability and brightness. Our findings will support the development of high-performance, optically driven solid-state quantum emitters for applications such as photonic quantum computing and quantum networks.

ACKNOWLEDGMENTS

This research was supported by the Natural Sciences and Engineering Research Council of Canada, Grant No. RGPIN-2020-06322, and the Internet of Things: Quantum Sensors Challenge Program at the National Research Council of Canada.

AUTHOR DECLARATIONS

Conflict of Interest

The authors have no conflicts to disclose.

Author Contributions

G. R. Wilbur and A. Binai-Motlagh contributed equally.

G. R. Wilbur: Formal analysis (equal); Investigation (equal); Methodology (equal); Software (equal); Writing – review & editing (supporting). **A. Binai-Motlagh:** Formal analysis (equal); Investigation (equal); Methodology (equal); Software (equal); Writing – review & editing (supporting). **A. Clarke:** Formal analysis (supporting); Investigation (supporting); Methodology (supporting); Software (supporting). **A. Ramachandran:** Formal analysis (supporting); Investigation (supporting); Methodology (supporting); Software (supporting); Writing – review & editing (supporting). **N. Milson:** Investigation (supporting); Methodology (supporting). **J. P. Healey:** Investigation (supporting); Methodology (supporting). **S. O’Neal:** Methodology (equal); Resources (equal). **D. G. Deppe:** Methodology (equal); Resources (equal). **K. C. Hall:** Conceptualization (lead); Formal analysis (lead); Funding acquisition (lead); Investigation (lead); Methodology (lead); Software (lead); Supervision (lead); Validation (lead); Writing – original draft (lead); Writing – review & editing (lead).

DATA AVAILABILITY

The data that support the findings of this study are available from the corresponding author upon reasonable request.

REFERENCES

- ¹ P. Kok, W. J. Munro, K. Nemoto, T. C. Ralph, J. P. Dowling, and G. J. Milburn, “Linear optical quantum computing with photonic qubits,” *Rev. Mod. Phys.* **79**, 135 (2007).
- ² A. Aspuru-Guzik and P. Walther, “Photonic quantum simulators,” *Nat. Phys.* **8**, 285 (2012).
- ³ S. Wehner, D. Elkouss, and R. Hanson, “Quantum internet: A vision for the road ahead,” *Science* **362**, 303 (2018).
- ⁴ J. Borregaard, H. Pichler, T. Schröder, M. D. Lukin, P. Lodahl, and A. S. Sørensen, “One-way quantum repeater based on near-deterministic photon-emitter interfaces,” *Phys. Rev. X* **10**, 021071 (2020).
- ⁵ J. Kołodyński, A. Máttar, P. Skrzypczyk, E. Woodhead, D. Cavalcanti, K. Banaszek, and A. Acín, *Quantum* **4**, 260 (2020).
- ⁶ X.-L. Chu, S. Götzinger, and V. Sandoghdar, “A single molecule as a high-fidelity photon gun for producing intensity-squeezed light,” *Nat. Photonics* **11**, 58 (2017).
- ⁷ H. Wang, J. Qin, S. Chen, M.-C. Chen, X. You, X. Ding, Y.-H. Huo, Y. Yu, C. Schneider, S. Höfling, M. Scully, C.-Y. Lu, and J.-W. Pan, “Observation of intensity squeezing in resonance fluorescence from a solid state device,” *Phys. Rev. Lett.* **125**, 153601 (2020).
- ⁸ A. J. Bennett, J. P. Lee, D. J. P. Ellis, T. Meany, E. Murray, F. F. Floether, J. P. Griffiths, I. Farrer, D. A. Ritchie, and A. J. Shields, “Cavity-enhanced coherent light scattering from a quantum dot,” *Sci. Adv.* **2**, 1501256 (2016).
- ⁹ M. Müller, H. Vural, C. Schneider, A. Rastelli, O. G. Schmidt, S. Höfling, and P. Michler, “Quantum-dot single-photon sources for entanglement-enhanced interferometry,” *Phys. Rev. Lett.* **118**, 257402 (2017).

- ¹⁰Y.-J. Wei, Y.-M. He, M.-C. Chen, Y.-N. Hu, Y. He, D. Wu, C. Schneider, M. Kamp, S. Höfling, C.-Y. Lu, and J.-W. Pan, "Deterministic and robust generation of single photons from a single quantum dot with 99.5% indistinguishability using adiabatic rapid passage," *Nano Lett.* **14**, 6515 (2014).
- ¹¹A. V. Kuhlmann, J. H. Prechtel, J. Houel, A. Ludwig, D. Reuter, A. D. Wieck, and R. J. Warburton, "Transform-limited single photons from a single quantum dot," *Nat. Commun.* **6**, 8204 (2015).
- ¹²N. Somaschi, V. Giesz, L. De Santis, J. C. Loredo, M. P. Almeida, G. Hornecker, S. L. Portalupi, T. Grange, C. Antón, J. Demory, C. Gómez, I. Sagnes, N. D. Lanzillotti-Kimura, A. Lemaitre, A. Auffeves, A. G. White, L. Lanco, and P. Senellart, "Near-optimal single-photon sources in the solid state," *Nat. Photonics* **10**, 340 (2016).
- ¹³X. Ding, Y. He, Z.-C. Duan, N. Gregersen, M.-C. Chen, S. Unsleber, S. Maier, C. Schneider, M. Kamp, S. Höfling, C.-Y. Lu, and J.-W. Pan, "On-demand single photons with high extraction efficiency and near-unity indistinguishability from a resonantly driven quantum dot in a micropillar," *Phys. Rev. Lett.* **116**, 020401 (2016).
- ¹⁴H. Wang, Z.-C. Duan, Y.-H. Li, S. Chen, J.-P. Li, Y.-M. He, M.-C. Chen, Y. He, X. Ding, C.-Z. Peng, C. Schneider, M. Kamp, S. Höfling, C.-Y. Lu, and J.-W. Pan, "Near-transform-limited single photons from an efficient solid-state quantum emitter," *Phys. Rev. Lett.* **116**, 213601 (2016).
- ¹⁵S. Gerhardt, J. Iles-Smith, D. P. S. McCutcheon, Y.-M. He, S. Unsleber, S. Betzold, N. Gregersen, J. Mørk, S. Höfling, and C. Schneider, "Intrinsic and environmental effects on the interference properties of a high-performance quantum dot single-photon source," *Phys. Rev. B* **97**, 195432 (2018).
- ¹⁶Y.-M. He, Y. He, Y.-J. Wei, D. Wu, M. Atatüre, C. Schneider, S. Höfling, M. Kamp, C.-Y. Lu, and J.-W. Pan, "On-demand semiconductor single-photon source with near-unity indistinguishability," *Nat. Nanotechnol.* **8**, 213 (2013).
- ¹⁷S. Unsleber, Y.-M. He, S. Gerhardt, S. Maier, C.-Y. Lu, J.-W. Pan, N. Gregersen, M. Kamp, C. Schneider, and S. Höfling, "Highly indistinguishable on-demand resonance fluorescence photons from a deterministic quantum dot micropillar device with 74% extraction efficiency," *Opt. Express* **24**, 8539 (2016).
- ¹⁸H. Wang, Y.-M. He, T.-H. Chung, H. Hu, Y. Yu, S. Chen, X. Ding, M.-C. Chen, J. Qin, X. Yang, R.-Z. Liu, Z.-C. Duan, J.-P. Li, S. Gerhardt, K. Winkler, J. Jurkat, L.-J. Wang, N. Gregersen, Y.-H. Huo, Q. Dai, S. Yu, S. Höfling, C.-Y. Lu, and J.-W. Pan, "Towards optimal single-photon sources from polarized microcavities," *Nat. Photonics* **13**, 770 (2019).
- ¹⁹N. Tömm, A. Javadi, N. O. Antoniadis, D. Najer, M. C. Löbl, A. R. Korsch, R. Schott, S. R. Valentin, A. D. Wieck, A. Ludwig, and R. J. Warburton, "A bright and fast source of coherent single photons," *Nat. Nanotechnol.* **16**, 399 (2021).
- ²⁰T. Huber, M. Davanco, M. Müller, Y. Shuai, O. Gazzano, and G. S. Solomon, "Filter-free single-photon quantum dot resonance fluorescence in an integrated cavity-waveguide device," *Optica* **7**, 380 (2020).
- ²¹R. Uppu, H. T. Eriksen, H. Thyrrstrup, A. D. Uğurlu, Y. Wang, S. Scholz, A. D. Wieck, A. Ludwig, M. C. Löbl, R. J. Warburton, P. Lodahl, and L. Midolo, "On-chip deterministic operation of quantum dots in dual-mode waveguides for a plug-and-play single-photon source," *Nat. Commun.* **11**, 3782 (2020).
- ²²A. Müller, E. B. Flagg, P. Bianucci, X. Y. Wang, D. G. Deppe, W. Ma, J. Zhang, G. J. Salamo, M. Xiao, and C. K. Shih, "Resonance fluorescence from a coherently driven semiconductor quantum dot in a cavity," *Phys. Rev. Lett.* **99**, 187402 (2007).
- ²³S. Ates, S. M. Ulrich, S. Reitzenstein, A. Löffler, A. Forchel, and P. Michler, "Post-selected indistinguishable photons from the resonance fluorescence of a single quantum dot in a microcavity," *Phys. Rev. Lett.* **103**, 167402 (2009).
- ²⁴F. Liu, A. J. Brash, J. O'Hara, L. M. P. P. Martins, C. L. Phillips, R. J. Coles, B. Royall, E. Clarke, C. Bentham, N. Prtljaga, I. E. Itskevich, L. R. Wilson, M. S. Skolnick, and A. M. Fox, "High Purcell factor generation of indistinguishable on-chip single photons," *Nat. Nanotechnol.* **13**, 835 (2018).
- ²⁵R. Uppu, F. T. Pedersen, Y. Wang, C. T. Olesen, C. Papon, X. Zhou, L. Midolo, S. Scholz, A. D. Wieck, A. Ludwig, and P. Lodahl, "Scalable integrated single-photon source," *Sci. Adv.* **6**, eabc8268 (2020).
- ²⁶Ł. Dusanowski, S.-H. Kwon, C. Schneider, and S. Höfling, "Near-unity indistinguishability single photon source for large-scale integrated quantum optics," *Phys. Rev. Lett.* **122**, 173602 (2019).
- ²⁷G. Kiršanskė, H. Thyrrstrup, R. S. Daveau, C. L. Dreeßen, T. Pregolato, L. Midolo, P. Tighineanu, A. Javadi, S. Stobbe, R. Schott, A. Ludwig, A. D. Wieck, S. I. Park, J. D. Song, A. V. Kuhlmann, I. Söllner, M. C. Löbl, R. J. Warburton, and P. Lodahl, "Indistinguishable and efficient single photons from a quantum dot in a planar nanobeam waveguide," *Phys. Rev. B* **96**, 165306 (2017).
- ²⁸S. E. Thomas, M. Billard, N. Coste, S. C. Wein, P. Priya, H. Ollivier, O. Krebs, L. Tazairt, A. Harouri, A. Lemaitre, I. Sagnes, C. Anton, L. Lanco, N. Somaschi, J. C. Loredo, and P. Senellart, "Bright polarized single-photon source based on a linear dipole," *Phys. Rev. Lett.* **126**, 233601 (2021).
- ²⁹K. H. Madsen, S. Ates, J. Liu, A. Javadi, S. M. Albrecht, I. Yeo, S. Stobbe, and P. Lodahl, "Efficient out-coupling of high-purity single photons from a coherent quantum dot in a photonic crystal cavity," *Phys. Rev. B* **90**, 155303 (2014).
- ³⁰M. Reindl, J. H. Weber, D. Huber, C. Schimpf, S. F. Covre da Silva, S. L. Portalupi, R. Trotta, P. Michler, and A. Rastelli, "Highly indistinguishable single photons from incoherently excited quantum dots," *Phys. Rev. B* **100**, 155420 (2019).
- ³¹D. Heinze, D. Breddermann, A. Zrenner, and S. Schumacher, "A quantum dot single-photon source with on-the-fly all-optical polarization control and timed emission," *Nat. Commun.* **6**, 8473 (2015).
- ³²M. Müller, S. Bounouar, K. D. Jöns, M. Glässl, and P. Michler, "On-demand generation of indistinguishable polarization-entangled photon pairs," *Nat. Photonics* **8**, 224 (2014).
- ³³H. Wang, H. Hu, T.-H. Chung, J. Qin, X. Yang, J.-P. Li, R.-Z. Liu, H.-S. Zhong, Y.-M. He, X. Ding, Y.-H. Deng, Q. Dai, Y.-H. Huo, S. Höfling, C.-Y. Lu, and J.-W. Pan, "On-demand semiconductor source of entangled photons which simultaneously has high fidelity, efficiency, and indistinguishability," *Phys. Rev. Lett.* **122**, 113602 (2019).
- ³⁴L. Schweickert, K. D. Jöns, K. D. Zeuner, S. F. Covre da Silva, H. Huang, T. Lettner, M. Reindl, J. Zichi, R. Trotta, A. Rastelli, and V. Zwiller, "On-demand generation of background-free single photons from a solid-state source," *Appl. Phys. Lett.* **112**, 093106 (2018).
- ³⁵Y. Chen, M. Zopf, R. Keil, F. Ding, and O. G. Schmidt, "Highly-efficient extraction of entangled photons from quantum dots using a broadband optical antenna," *Nat. Commun.* **9**, 2994 (2018).
- ³⁶L. Hanschke, K. A. Fischer, S. Appel, D. Lukin, J. Wierzbowski, S. Sun, R. Trivedi, J. Vučković, J. J. Finley, and K. Müller, "Quantum dot single-photon sources with ultra-low multi-photon probability," *npj Quantum Inf.* **4**, 43 (2018).
- ³⁷J. Liu, R. Su, Y. Wei, B. Yao, S. F. Covre da Silva, Y. Yu, J. Iles-Smith, K. Srinivasan, A. Rastelli, J. Li, and X. Wang, "A solid-state source of strongly entangled photon pairs with high brightness and indistinguishability," *Nat. Nanotechnol.* **14**, 586 (2019).
- ³⁸D. Huber, M. Reindl, Y. Huo, H. Huang, J. S. Wildmann, O. G. Schmidt, A. Rastelli, and R. Trotta, "Highly indistinguishable and strongly entangled photons from symmetric GaAs quantum dots," *Nat. Commun.* **8**, 15506 (2017).
- ³⁹H. Jayakumar, A. Predojević, T. Huber, T. Kauten, G. S. Solomon, and G. Weihs, "Deterministic photon pairs and coherent optical control of a single quantum dot," *Phys. Rev. Lett.* **110**, 135505 (2013).
- ⁴⁰K. D. Jöns, L. Schweickert, M. A. M. Versteegh, D. Dalacu, P. J. Poole, A. Gulinatti, A. Giudice, V. Zwiller, and M. E. Reimer, "Bright nanoscale source of deterministic entangled photon pairs violating Bell's inequality," *Sci. Rep.* **7**, 1700 (2017).
- ⁴¹O. Gazzano, S. Michaelis de Vasconcellos, C. Arnold, A. Nowak, E. Galopin, I. Sagnes, L. Lanco, A. Lemaitre, and P. Senellart, "Bright solid-state sources of indistinguishable single photons," *Nat. Commun.* **4**, 1425 (2013).
- ⁴²T. Huber, A. Predojević, D. Föger, G. Solomon, and G. Weihs, "Optimal excitation conditions for indistinguishable photons from quantum dots," *New J. Phys.* **17**, 123025 (2015).
- ⁴³H. Huang, S. Manna, C. Schimpf, M. Reindl, X. Yuan, Y. Zhang, S. F. Covre da Silva, and A. Rastelli, "Bright single photon emission from quantum dots embedded in a broadband planar optical antenna," *Adv. Opt. Mater.* **9**, 2001490 (2021).
- ⁴⁴D. H. Ahn, Y. D. Jang, J. S. Baek, C. Schneider, S. Höfling, and D. Lee, "A broad-band planar-microcavity quantum-dot single-photon source with a solid immersion lens," *Appl. Phys. Lett.* **118**, 174001 (2021).
- ⁴⁵J. Claudon, J. Bleuse, N. S. Malik, M. Bazin, P. Jaffrennou, N. Gregersen, C. Sauvan, P. Lalanne, and J.-M. Gérard, "A highly efficient single-photon source based on a quantum dot in a photonic nanowire," *Nat. Photonics* **4**, 174 (2010).

- ⁴⁶J. Jurkat, M. Moczala-Dusanowska, M. A. Jacobsen, A. Predojević, T. Huber, N. Gregersen, S. Höfling, and C. Schneider, "Technological implementation of a photonic Bier-Glass cavity," *Phys. Rev. Mater.* **5**, 064603 (2021).
- ⁴⁷M. E. Reimer, G. Bulgarini, N. Akopian, M. Hocevar, M. B. Bavinck, M. A. Verheijen, E. P. A. M. Bakkers, L. P. Kouwenhoven, and V. Zwiller, "Bright single-photon sources in bottom-up tailored nanowires," *Nat. Commun.* **3**, 737 (2012).
- ⁴⁸M. Arcari, I. Söllner, A. Javadi, S. Lindskov Hansen, S. Mahmoodian, J. Liu, H. Thyrrstrup, E. H. Lee, J. D. Song, S. Stobbe, and P. Lodahl, "Near-unity coupling efficiency of a quantum emitter to a photonic crystal waveguide," *Phys. Rev. Lett.* **113**, 093603 (2014).
- ⁴⁹T. Huber, A. Predojević, H. Zoubi, H. Jayakumar, G. S. Solomon, and G. Weihs, "Measurement and modification of biexciton-exciton time correlations," *Opt. Express* **21**, 9890 (2013).
- ⁵⁰J. Yan, S. Liu, X. Lin, Y. Ye, J. Yu, L. Wang, Y. Yu, Y. Zhao, Y. Meng, X. Hu, D. Wang, C. Jin, and F. Liu, "Double-pulse generation of indistinguishable single photons with optically controlled polarization," *Nano Lett.* **22**, 1483 (2022).
- ⁵¹Y. Wei, S. Liu, X. Li, Y. Yu, X. Su, S. Li, S. Xiang, H. Liu, H. Hao, H. Ni, S. Yu, Z. Niu, J. Liu, and X. Wang, "Tailoring solid-state single-photon sources with stimulated emissions," *Nat. Nanotechnol.* **17**, 470 (2022).
- ⁵²Y.-M. He, H. Wang, C. Wang, M.-C. Chen, X. Ding, J. Qin, Z.-C. Duan, S. Chen, J.-P. Li, R.-Z. Liu, C. Schneider, M. Atatüre, S. Höfling, C.-Y. Lu, and J.-W. Pan, "Coherently driving a single quantum two-level system with dichromatic laser pulses," *Nat. Phys.* **15**, 941 (2019).
- ⁵³Z. X. Koong, E. Scerri, M. Rambach, M. Cygorek, M. Brotons-Gisbert, R. Picard, Y. Ma, S. I. Park, J. D. Song, E. M. Gauger, and B. D. Gerardot, "Coherent dynamics in quantum emitters under dichromatic excitation," *Phys. Rev. Lett.* **126**, 047403 (2021).
- ⁵⁴T. K. Bracht, M. Cosacchi, T. Seidelmann, M. Cygorek, A. Vagov, V. M. Axt, T. Heindel, and D. E. Reiter, "Swing-up of quantum emitter population using detuned pulses," *PRX Quantum* **2**, 040354 (2021).
- ⁵⁵C. Gustin and S. Hughes, "Influence of electron-phonon scattering for an on-demand quantum dot single-photon source using cavity-assisted adiabatic passage," *Phys. Rev. B* **96**, 085305 (2017).
- ⁵⁶R. Mathew, E. Dilcher, A. Gamouras, A. Ramachandran, H. Y. S. Yang, S. Freisem, D. Deppe, and K. C. Hall, "Subpicosecond adiabatic rapid passage on a single semiconductor quantum dot: Phonon-mediated dephasing in the strong-driving regime," *Phys. Rev. B* **90**, 035316 (2014).
- ⁵⁷S. Lüker and D. E. Reiter, "A review on optical excitation of semiconductor quantum dots under the influence of phonons," *Semicond. Sci. Technol.* **34**, 063002 (2019).
- ⁵⁸D. Wigger, C. Schneider, S. Gerhardt, M. Kamp, S. Höfling, T. Kuhn, and J. Kasprzak, "Rabi oscillations of a quantum dot exciton coupled to acoustic phonons: Coherence and population readout," *Optica* **5**, 1442 (2018).
- ⁵⁹A. J. Ramsay, A. V. Gopal, E. M. Gauger, A. Nazir, B. W. Lovett, A. M. Fox, and M. S. Skolnick, "Damping of exciton Rabi rotations by acoustic phonons in optically excited InGaAs/GaAs quantum dots," *Phys. Rev. Lett.* **104**, 017402 (2010).
- ⁶⁰A. J. Ramsay, T. M. Godden, S. J. Boyle, E. M. Gauger, A. Nazir, B. W. Lovett, A. M. Fox, and M. S. Skolnick, "Phonon-induced Rabi-frequency renormalization of optically driven single InGaAs/GaAs quantum dots," *Phys. Rev. Lett.* **105**, 177402 (2010).
- ⁶¹A. Vagov, M. D. Croitoru, V. M. Axt, T. Kuhn, and F. M. Peeters, "Nonmonotonic field dependence of damping and reappearance of Rabi oscillations in quantum dots," *Phys. Rev. Lett.* **98**, 227403 (2007).
- ⁶²M. Atatüre, D. Englund, N. Vamivakas, S.-Y. Lee, and J. Wrachtrup, "Material platforms for spin-based photonic quantum technologies," *Nat. Rev. Mater.* **3**, 38 (2018).
- ⁶³M. M. T. Loy, "Observation of population inversion by optical adiabatic rapid passage," *Phys. Rev. Lett.* **32**, 814 (1974).
- ⁶⁴V. S. Malinovsky and J. L. Krause, "General theory of population transfer by adiabatic rapid passage with intense, chirped laser pulses," *Eur. Phys. J. D* **14**, 147 (2001).
- ⁶⁵B. W. Shore, *Manipulating Quantum Structures Using Laser Pulses* (Cambridge University Press, New York, 2011), pp. 513–521.
- ⁶⁶A. Ramachandran, J. Fraser-Leach, S. O'Neal, D. G. Deppe, and K. C. Hall, "Experimental quantification of the robustness of adiabatic rapid passage for quantum state inversion in semiconductor quantum dots," *Opt. Express* **29**, 41766 (2021).
- ⁶⁷C.-M. Simon, T. Belhadj, B. Chatel, T. Amand, P. Renucci, A. Lemaitre, O. Krebs, P. A. Dalgarno, R. J. Warburton, X. Marie, and B. Urbaszek, "Robust quantum dot exciton generation via adiabatic rapid passage with frequency-swept optical pulses," *Phys. Rev. Lett.* **106**, 166801 (2011).
- ⁶⁸Y. Wu, I. M. Piper, M. Ediger, P. Brereton, E. R. Schmidgall, P. R. Eastham, M. Hugues, M. Hopkinson, and R. T. Phillips, "Population inversion in a single InGaAs quantum dot using the method of adiabatic rapid passage," *Phys. Rev. Lett.* **106**, 067401 (2011).
- ⁶⁹A. Gamouras, R. Mathew, S. Freisem, D. G. Deppe, and K. C. Hall, "Simultaneous deterministic control of distant qubits in two semiconductor quantum dots," *Nano Lett.* **13**, 4666 (2013).
- ⁷⁰T. Kaldewey, S. Lüker, A. V. Kuhlmann, S. R. Valentin, A. Ludwig, A. D. Wieck, D. E. Reiter, T. Kuhn, and R. J. Warburton, "Coherent and robust high-fidelity generation of a biexciton in a quantum dot by rapid adiabatic passage," *Phys. Rev. B* **95**, 161302(R) (2017).
- ⁷¹T. Kaldewey, S. Lüker, A. V. Kuhlmann, S. R. Valentin, J.-M. Chauveau, A. Ludwig, A. D. Wieck, D. E. Reiter, T. Kuhn, and R. J. Warburton, "Demonstrating the decoupling regime of the electron-phonon interaction in a quantum dot using chirped pulse optical excitation," *Phys. Rev. B* **95**, 241306(R) (2017).
- ⁷²A. Ramachandran, G. R. Wilbur, S. O'Neal, D. G. Deppe, and K. C. Hall, "Suppression of decoherence tied to electron-phonon coupling in telecom-compatible quantum dots: Low-threshold reappearance regime for quantum state inversion," *Opt. Lett.* **45**, 6498 (2020).
- ⁷³A. Gamouras, R. Mathew, and K. C. Hall, "Optically engineered ultrafast pulses for controlled rotations of exciton qubits in semiconductor quantum dots," *J. Appl. Phys.* **112**, 014313 (2012).
- ⁷⁴R. Mathew, C. E. Pryor, M. E. Flatté, and K. C. Hall, "Optimal quantum control for conditional rotation of exciton qubits in semiconductor quantum dots," *Phys. Rev. B* **84**, 205322 (2011).
- ⁷⁵A. J. Ramsay, T. M. Godden, S. J. Boyle, E. M. Gauger, A. Nazir, B. W. Lovett, A. V. Gopal, A. M. Fox, and M. S. Skolnick, "Effect of detuning on the phonon induced dephasing of optically driven InGaAs/GaAs quantum dots," *J. Appl. Phys.* **109**, 102415 (2011).
- ⁷⁶Note that our sample is a simple flat wafer, which reduces collection efficiency; however, our scheme could be implemented in practice using a nanowire or other photonic structure to optimize brightness.
- ⁷⁷See, for example, <https://www.thorlabs.com/> and <https://alluxa.com/>.
- ⁷⁸Z.-X. Koong, G. Ballesteros-Garcia, R. Proux, D. Dalacu, P. J. Poole, and B. D. Gerardot, "Multiplexed single photons from deterministically positioned nanowire quantum dots," *Phys. Rev. Appl.* **14**, 034011 (2020).
- ⁷⁹M. Glässl, A. M. Barth, and V. M. Axt, "Proposed robust and high-fidelity preparation of excitons and biexcitons in semiconductor quantum dots making active use of phonons," *Phys. Rev. Lett.* **110**, 147401 (2013).
- ⁸⁰P.-L. Ardel, L. Hanschke, K. A. Fischer, K. Müller, A. Kleinkauf, M. Koller, A. Bechtold, T. Simmet, J. Wierzbowski, H. Riedl, G. Abstreiter, and J. J. Finley, "Dissipative preparation of the exciton and biexciton in self assembled quantum dots on picosecond time scales," *Phys. Rev. B* **90**, 241404(R) (2014).